Slow delocalization of particles in many-body localized phases

Maximilian Kiefer-Emmanouilidis,[1,2] Razmik Unanyan,[1] Michael Fleischhauer,[1] and Jesko Sirker[2,3]

[1]*Department of Physics and Research Center OPTIMAS, University Kaiserslautern, 67663 Kaiserslautern, Germany*
[2]*Department of Physics and Astronomy, University of Manitoba, Winnipeg R3T 2N2, Canada*
[3]*Manitoba Quantum Institute, University of Manitoba, Winnipeg R3T 2N2, Canada*

We have recently shown that the logarithmic growth of the entanglement entropy following a quantum quench in a many-body localized phase is accompanied by a slow growth of the number entropy $S_N \sim \ln \ln t$. Here we provide an in-depth numerical study of $S_N(t)$ for the disordered Heisenberg chain and show that this behavior is not transient and persists even for very strong disorder. Calculating the truncated Rényi number entropy $S_N^{(\alpha)}(t) = (1-\alpha)^{-1} \ln \sum_n p^\alpha(n)$ for $\alpha \ll 1$ and $p(n) > p_c$—which is sensitive to large number fluctuations occurring with low probability—we demonstrate that the particle number distribution $p(n)$ in one half of the system has a continuously growing tail. This indicates a slow but steady increase in the number of particles crossing between the partitions in the interacting case and is in sharp contrast to Anderson localization for which we show that $S_N^{(\alpha \to 0)}(t)$ saturates for any cutoff $p_c > 0$. We show, furthermore, that the growth of S_N is *not* the consequence of rare states or rare regions but rather represents typical behavior. These findings indicate that the interacting system is never fully localized even for very strong but finite disorder.

I. INTRODUCTION

In a one-dimensional system of free particles with short-range hoppings, even the smallest amount of potential disorder leads to a localization of the single-particle wave functions, a phenomena termed Anderson localization [1–3]. A question which has remained open for more than 50 years is whether or not localization is also possible in an interacting many-body system. This question has been put back to the forefront of research in condensed-matter physics by a seminal work by Basko, Aleiner, and Altshuler arguing perturbatively that at weak interactions a metal-insulator transition, i.e., a many-body localization (MBL) transition, will occur at some finite temperature T_c [4]. This paper has sparked a number of studies of possible ergodic-MBL transitions in disordered lattice models. The most studied of these models is the spin-1/2 Heisenberg chain with local magnetic fields drawn from a box distribution [5–17], which is equivalent to the fermionic t-V model with potential disorder. The results have been interpreted in terms of an ergodic-MBL transition at finite disorder strength. Under the assumption of limited level attraction, perturbative arguments for the stability of a MBL phase in spin chains have been put forward [18,19] but a rigorous proof is lacking. Very recently, numerical studies have cast some doubt on the stability of the MBL phase in the thermodynamic limit [20–25]. However, the interpretation of these results is still a matter of debate [26–30].

Another recent development is the study of symmetry-resolved entanglement measures [31–36]. For a system with particle number conservation, the von Neumann entanglement entropy S can be split into two contributions,

$$S = S_N + S_c, \quad S_N = -\sum p(n) \ln p(n),$$

$$S_c = -\sum_n p(n) \mathrm{tr}[\rho(n) \ln \rho(n)]. \tag{1}$$

Here S_N is the number entropy which is entirely characterized by the probability $p(n)$ to find n particles in the considered subsystem. S_c is the configurational entropy with $\rho(n)$ being the block of the reduced density matrix with particle number n. Using symmetries is, on one hand, of fundamental interest from a quantum information perspective to calculate the amount of operational entanglement which is available [31,37–39], it is, on the other hand, also helpful to understand how much of the entanglement is caused by particle fluctuations and how much is due to the superposition of different configurations in a sector of constant particle number. The usefulness of this approach has recently been demonstrated in a cold-atomic gas experiment where entanglement following a quench in a one-dimensional Aubry-André Bose-Hubbard model was studied [33]. The experimental results have been interpreted in terms of a number entropy which saturates and a configurational entropy which then continues growing logarithmically on top of the constant number entropy [see Fig. 1(a)]. The resulting logarithmic growth of the total entanglement entropy has been confirmed in several numerical studies [40–44]. The behavior of the number entropy S_N, however, has received much less attention. Very recently, we have shown that in the numerically accessible time regime the logarithmic growth of entanglement in the MBL phase is accompanied by a growth $S_N \sim \ln \ln t$ of the number entropy [see Fig. 1(b)] [24,25]. If this behavior does persist in the thermodynamic limit for all finite disorder strengths, then the MBL phase would ultimately not be localized and the system would likely always remain ergodic.

The purpose of this paper is to further study the two scenarios for the entanglement evolution in MBL phases, shown schematically in Fig. 1. To do so, we will carefully study the timescales where the scaling behavior holds as well as the dis-
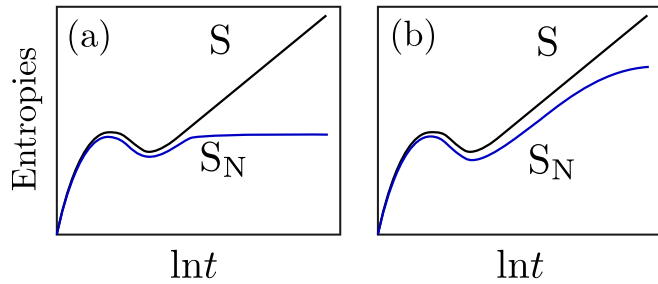
FIG. 1. (a) The standard MBL scenario: The number entropy saturates. A further logarithmic increase in the entanglement entropy is caused entirely by the configurational entropy. (b) Alternative scenario: The number entropy never saturates. The logarithmic increase in the total entanglement coexists with a $S_N \sim \ln \ln t$ increase in the number entropy.

tributions of the total entanglement entropy and of the number entropy. It has also been suggested recently by Luitz and Bar Lev [27] that the increase in the number entropy observed in our previous publication Ref. [25] might be a result of disorder strengths that were still relatively close to the transition point. In order to address this point, we will extend our numerical study to disorder strengths up to twice of what is believed to be the critical value. It is known that on the localized side but still close to the ergodic-MBL transition, rare regions with less disorder can cause a very slow dynamics [45,46] and can destabilize the MBL phase in small systems. In order to exclude such a scenario we will compare the average with the median number entropy and show that the observed growth of the number entropy is *not* a consequence of rare initial states or rare regions.

To further investigate if the observed slow growth of the number entropy is transient, we study the time evolution of the (discrete) probability distribution $p(n,t)$. If MBL is associated with a very slow formation of localized states, there could be a long transient time period where probabilities redistribute in a very narrow range of particle numbers, whereas larger fluctuations are strictly suppressed. The number entropy is not sufficiently sensitive to large particle number fluctuations occurring with small probability and, thus, cannot unambiguously exclude such a scenario. A much more sensitive measure are the number Rényi entropies,

$$S_N^{(\alpha)} = (1-\alpha)^{-1} \ln \sum_{n=0}^{\infty} p^{\alpha}(n), \qquad (2)$$

with $\alpha \ll 1$. The family of Rényi entropies provides information about different characteristics of the probability distribution. $S_N^{(1)} = -\sum_n p(n) \ln p(n)$, for example, is the well-known Shannon entropy. For growing values of α the Rényi entropies are increasingly determined by the largest probability values. $S_N^{(\infty)} = -\ln p_{\max}(n)$, in particular, is given by the logarithm of the maximum probability. For decreasing values of $\alpha \ll 1$, $S_N^{(\alpha)}$ becomes increasingly sensitive to all nonvanishing probabilities including those that are small. Taking the limit $\alpha \to 0$, $S_N^{(\alpha)}$ gives the so-called Hartley number entropy, which essentially counts all values of n which have a nonvanishing probability $p(n)$. In order for the Hartley entropy to become a useful physical quantity to investigate the properties of $p(n)$ one has to introduce a cutoff probability

$p_c > 0$. E.g., if $p(n) > p_c$ for M values of n, then $S_N^{(0)} = \ln M$. If the system is localized then the truncated Hartley entropy for a system in the thermodynamic limit has to saturate for any cutoff p_c to a value that depends on p_c but which is much below the equipartition value, corresponding to a fully thermalized state.

Our paper is organized as follows: In Sec. II we introduce the model and notation and also discuss the numerical methods and the averaging procedure. In Sec. III we then present the results of our numerical investigations for the entanglement and number entropy. The section is subdivided into two subsections, dealing with the coexistence of the growth of S and S_N and a comparison between the average and the median, and the distributions of entanglement for different realizations, respectively. The results for the Hartley number entropy are discussed in Sec. IV. In Sec. V we present our conclusions and discuss some of the remaining open questions.

II. MODEL AND METHODS

We concentrate here on the isotropic Heisenberg model in the fermionic representation (t-V model),

$$H = -J \sum_j \{(c_j^\dagger c_{j+1} + \text{H.c.}) + D_j n_j + V n_j n_{j+1}\}, \qquad (3)$$

with nearest-neighbor interaction $V = 2J$. We assume a half-filled system and draw random values of the local potential from a box distribution $D_j \in [-D/2, D/2]$. Throughout, we are using open boundary conditions. Note that in the notation used here, $D_j = 4h_j$ where h_j are the local magnetic fields in the spin representation used, for example, in Refs. [6–8]. We are interested in the growth of entanglement following a quantum quench from a random product state $|\Psi_0\rangle$. This state is then time evolved, $|\Psi(t)\rangle = \exp(-iHt)|\Psi_0\rangle$. We set $J = 1$ throughout this paper.

For system sizes $L \leqslant 14$ we use exact diagonalizations of the Hamiltonian matrix to obtain the time-evolved state $|\Psi(t)\rangle$. We then calculate the reduced density matrix by tracing out half of the system $\rho = \text{tr}_A |\Psi(t)\rangle\langle\Psi(t)|$ and calculate the number distribution $p(n,t)$. Typically, we pick 10 000 random disorder configurations, and for each disorder configuration we average over 50 random half-filled initial product states. To avoid any possible issues due to the double precision limitations of standard exact diagonalizations [47], we limit ourselves to system sizes where the saturation times remain $\lesssim 10^{14}$.

As a complementary method, we use a Trotter-Suzuki decomposition of the time-evolution operator [48–50]. This allows to reach larger system sizes; we restrict ourselves here to $L \leqslant 24$—for even larger systems the computational cost of calculating several thousand samples becomes prohibitive. Since the Trotter error of the decomposition accumulates over time, the simulation times for the chosen Trotter parameter $\delta t \sim 10^{-4}$ are limited to $t \lesssim 10^3$. Here, we typically average over 1500 disorder realizations for $D \leqslant 28$ and 2000 for $D > 28$ and pick a random initial product state for each realization. We note that the various entropies are calculated first for each sample separately and are then, in a second step, either averaged over all realizations or used to calculate the median.
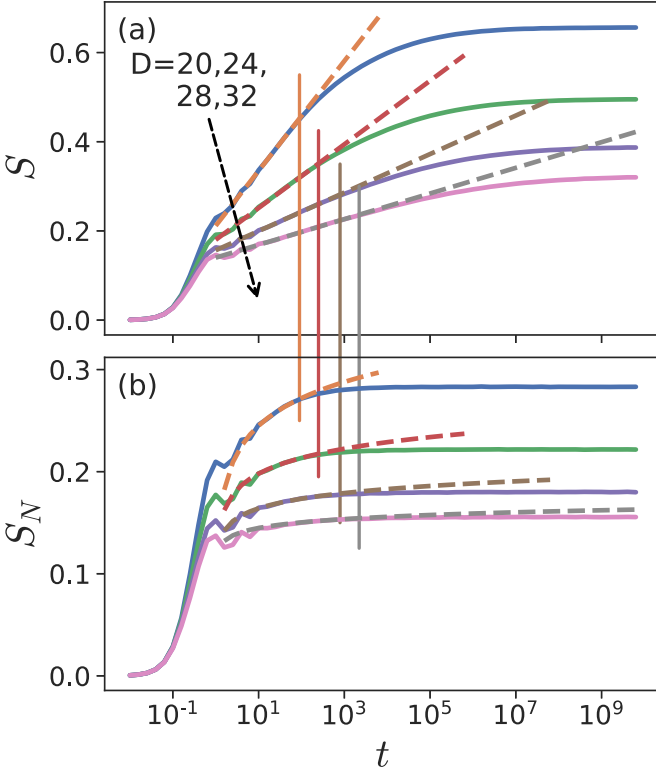
FIG. 2. (a) Entanglement entropy, and (b) number entropy for $L = 14$ and different disorder strengths $D > D_c$. The dashed lines are logarithmic (double logarithmic) fits, respectively. In all cases, finite-size saturation sets in at the same timescale (marked by vertical lines) in both quantities.
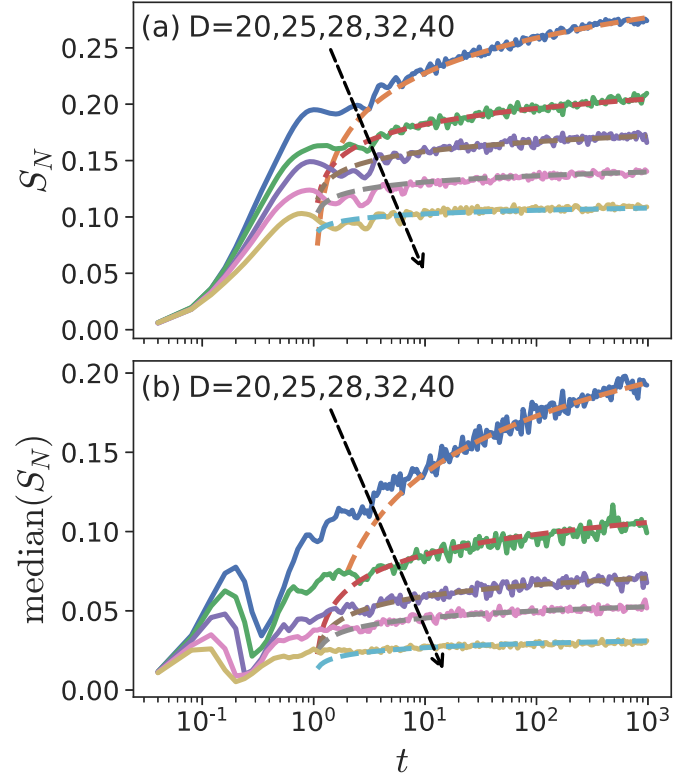

FIG. 3. Averaged number entropy [panel (a)] and median number entropy [panel (b)] for $L = 24$ and different disorder strengths $D > D_c$. The $S_N \sim \ln \ln t$ scaling (represented by the dashed-line fits) persists for all disorder strengths in *both* quantities up to the longest times reached in our simulations.

III. ENTANGLEMENT ENTROPY AND NUMBER ENTROPY

Here we present and analyze the results for the entanglement and number entropies obtained by the numerical simulations described above. We provide evidence that the unbounded growth of the number entropy persists even deep in the MBL phase and that it is associated with subexponential tails in the probability distribution $p(S_N)$ of the number entropy, which grow in time. We also show that not only the average number entropy grows as $S_N \sim \ln \ln t$, but also the median number entropy, providing evidence that the observed behavior is typical and not due to rare cases.

A. Growth of $S(t)$ and $S_N(t)$

First, we want to demonstrate that the $S \sim \ln t$ growth of the entanglement entropy and the $S_N \sim \ln \ln t$ growth of the number entropy are intimately related and persist over the same timescales, only limited by the considered system size. Second, we want to demonstrate that this behavior is not restricted to a narrow range of disorder strengths near the localization transition but is also present deep in the MBL phase. Previous numerical calculations put the critical disorder in the range of $D_c \sim 14 \cdots 17$. In Fig. 2, we therefore present results for disorder strengths up to about twice the critical value. The main point we want to make is that both $S(t)$ and $S_N(t)$ start to saturate due to the finite size of the

system at *the same timescale.* We never find a case where S_N starts to saturate whereas S continues to grow logarithmically as would be expected in the standard scenario, Fig. 1(a). We find, furthermore, that a perfect $S_N \sim \ln \ln t$ scaling holds up to the largest simulation times even at very large disorder, see Fig. 3(a). Since there is still some debate about the precise value of the critical disorder strength for the onset of MBL, one could argue that our results in Ref. [25] might only be valid close to the transition point [27]. Our new results clearly show that this is not the case.

An important question then is what causes the slow growth of the number entropy. In Ref. [46] it has been argued that rare thermal regions in the localized phase can dominate its low-frequency response. To investigate whether or not the observed growth is related to rare initial states or rare disorder configurations leading to rare thermal inclusions, we show in Fig. 3(b) the median number entropy. This quantity is defined by sorting the number entropies for each realization in terms of magnitude at a given point in time and then choosing the value in the middle for an odd number of realizations or the average of the two middle values for an even number of realizations. The answer is unambiguous: The median number entropy shows the same double logarithmic growth in time as the average number entropy. We conclude that the observed growth is not the consequence of rare regions but rather represents the typical behavior of the number entropy. The scenarios discussed in Ref. [46] do not explain our

observations: We find that the short time rather then the long time behavior is strongly influenced by rare nontypical samples. When comparing Fig. 3(a) with Fig. 3(b) we see that the main qualitative difference is a suppression of the initial approximatively logarithmic increase in the median as compared to the average number entropy. A natural explanation is that rare regions with little disorder (called "thermal regions" in Ref. [46]) are responsible. Indeed, we have shown that in the ergodic phase at small disorder $S_N \sim \ln t$ [25]. Excluding rare configurations from the average as we do when calculating the median therefore strongly reduces the number entropy at short times—and, thus, also the overall values for all times—but does not change the scaling at long times.

B. Variance of entropies and entropy distribution functions

The numerical study of disordered systems requires a careful sampling of disorder realizations. So far, we have either considered averages over all realizations or have calculated the median. As pointed out in Ref. [27], it is, however, useful to consider also the probability distributions of these entropies with respect to the different realizations for a deeper understanding of the underlying physics. In fact, numerical studies in Ref. [27] have shown that whereas the variance of the asymptotic entanglement entropy ΔS approaches a constant value with increasing system size, the corresponding value of the number entropy ΔS_N decreases. In addition, it was shown that the probability distribution $p(S)$ of the entanglement entropy for a given system size L and large disorder has an exponential tail. In contrast, the probability distribution of the corresponding number entropy $p(S_N)$ shows a sharp cutoff at about $\ln(3)$, corresponding to a single-particle hopping back and forth across the boundary between the two halves of the system. Both findings could be taken as an indication that there is no particle redistribution deep in the MBL phase beyond the level of a single particle and that the increase in the entanglement entropy is solely due to configurational entanglement. The latter would also imply that the asymptotic relation between entanglement and number entropies derived in Ref. [24] for noninteracting systems and demonstrated to hold also for interacting particles in Ref. [25] of the form

$$S_N \sim \frac{1}{D^\nu} \ln S + \gamma \qquad (4)$$

ceases to hold deep in the MBL phase. Here $\nu > 0$ is an exponent of the order of unity. In the following we argue that this interpretation is too naive. The behavior of the probability distribution of entropies, observed in Ref. [27], is fully consistent with the relation (4) as it implies a subexponential tail of $p(S_N)$.

First, by assuming a small variation of the entanglement entropy from its average value $\overline{S}$, i.e., $S = \overline{S} + \Delta S$ and using Eq. (4), we find

$$\overline{S}_N + \Delta S_N \sim \frac{1}{D^\nu}\left[\ln(\overline{S}) + \ln\left(1 + \frac{\Delta S}{\overline{S}}\right)\right] + \gamma$$

$$\approx \frac{1}{D^\nu}\ln(\overline{S}) + \frac{1}{D^\nu}\frac{\Delta S}{\overline{S}} + \gamma. \qquad (5)$$

From this we can read off the variance of the number entropy. Using, furthermore, the scaling of the average entanglement
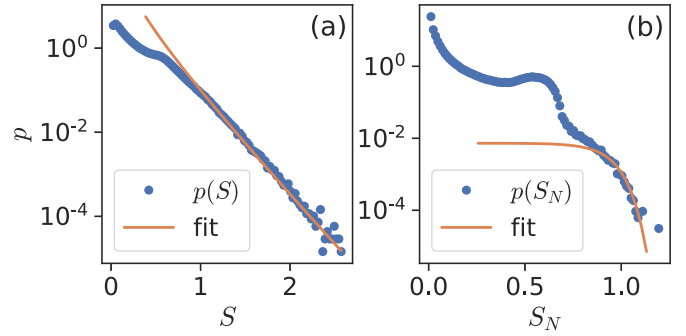

FIG. 4. Distribution of saturation values for $D = 40$ and $L = 16$. (a) von Neumann entropy S and (b) number entropy S_N. Symbols denote numerical data from Ref. [27], orange lines are fits, see the text.

entropy with system size $\overline{S} \sim L/D$ [51] we obtain $\Delta S_N \sim \Delta S/(D^\nu \overline{S}) \sim \Delta S/L$. The variance of the number entropy, therefore, decreases with increasing system size. There is, thus, no contradiction between the results in Ref. [27] and relation (4).

The authors of Ref. [27] found, furthermore, that the probability distribution of the asymptotic entanglement entropy in a finite system of length L has an exponential tail, which we fit as $p(S) \sim \exp(-2DS/L)/S$. This is shown in Fig. 4(a) where the distributions are based on the data from Ref. [27] and the fit is based on the relation above. Note that the prefactor in the exponent is in agreement with the asymptotic scaling $S \sim L/D$ found in Ref. [51]. If we plug Eq. (4) into $p(S)$ we find, using $dS_N \sim dS/S$,

$$p(S_N) \sim \exp\left\{-\frac{2D}{L}\exp\left[\frac{D}{4}(S_N - \gamma)\right]\right\}. \qquad (6)$$

This asymptotic expression shows a sharp cutoff for large values of D as soon as S_N exceeds γ. Figure 4(b) shows a comparison between the numerical data for $p(S_N)$ from Ref. [27] and the prediction (6) with γ used as a fitting parameter. The agreement is good. Thus, the seemingly sharp drop off of the probability distribution $p(S_N)$ does not contradict the relation between number and entanglement entropies found in Ref. [25] and is not a sufficient indicator for a complete suppression of particle transport beyond the level of a single particle.

Finally we note that the presence of a seemingly sharp drop in the probability distribution $p(S_N)$ is consistent with the *absence of localization* in other, exactly solvable models of noninteracting fermions. The case of free fermions on a lattice with off-diagonal (bond) disorder is discussed in Appendix A. This model is known to be not fully localized, but the probability distributions of the entropies show qualitatively the same behavior as for the disordered Heisenberg chain. We conclude that the features of the probability distributions for the entanglement and number entropy found in Ref. [27] do not contradict the relation $S_N \sim \ln S$ and are, therefore, not sufficient indicators for localization.
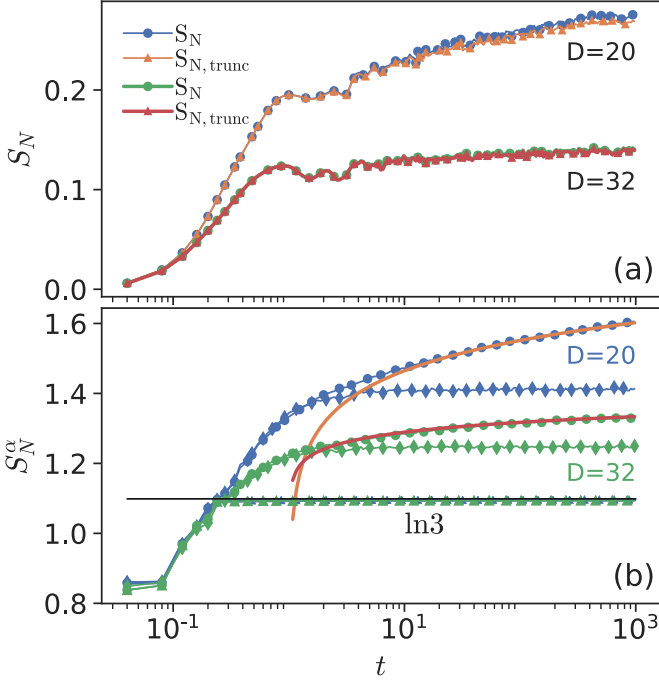
FIG. 5. (a) S_N for the full and the truncated distribution $p(n)$ where only contributions from $p(n_{\max})$, $p(n_{\max} \pm 1)$ are taken into account. (b) Rényi number entropies $S_N^{(\alpha)}$ for $\alpha = 0.001$ (circles) and double logarithmic fits (lines). Also shown is the Anderson case (diamonds), i.e., Eq. (3) with $V = 0$. $p(n)$ is truncated at $p_c = 10^{-10}$. The full entropies are compared to those where only $p(n_{\max})$ and $p(n_{\max} \pm 1)$ are taken into account (triangles). The latter approach the maximum value of ln 3.

FIG. 6. Rényi number entropy $S_N^{(\alpha)}(t)$ for $\alpha = 0.001$, $D = 32$, and different values of p_c. $S_N^{(\alpha)}$ increases with a decreasing cutoff value, leading effectively to a simple constant shift. For the Anderson case (diamonds) $S_N^{(\alpha)}(t)$ always saturates whereas $S_N^{(\alpha)} \sim \ln \ln t$ in the MBL case (circles).

IV. HARTLEY NUMBER ENTROPY AND NUMBER DISTRIBUTION

The pronounced drop off of $p(S_N)$ shown in Fig. 4 at $S_N \sim \ln 3 \approx 1.098$ could be taken as an indication that at sufficiently long times only a single particle fluctuates between the two halves of the system. If the system is localized, one expects that the probability distribution of particle numbers $p(n)$ in one partition for a given realization and initial state develops a sharp maximum at some value $n_{\max}$ in the thermodynamic limit after a transient. Thus, allowing fluctuations of a single particle one would expect nonvanishing probabilities only for the three values of n, $n = n_{\max}$, and $n = n_{\max} \pm 1$, limiting the number entropy to values less than ln 3. Since the number entropy does not exceed ln 3 in our simulations at strong disorder, a possible scenario consistent with the standard picture of MBL would be a long transient redistribution of probabilities within the restricted range $n_{\max} \pm 1$.

To assess the possibility of such a strictly bounded redistribution of probabilities, we have calculated the time evolution of S_N from a truncated distribution taking into account only the values $p(n_{\max})$ and $p(n_{\max} \pm 1)$. Figure 5(a) shows a comparison of the full with the truncated number entropy for two different disorder strengths. One recognizes—in particular, for the larger disorder value—that S_N in this regime is indeed dominated by those three probabilities. The number entropy is, however, insensitive to the dynamics in the tails of the probability distribution. Due to the extremely slow
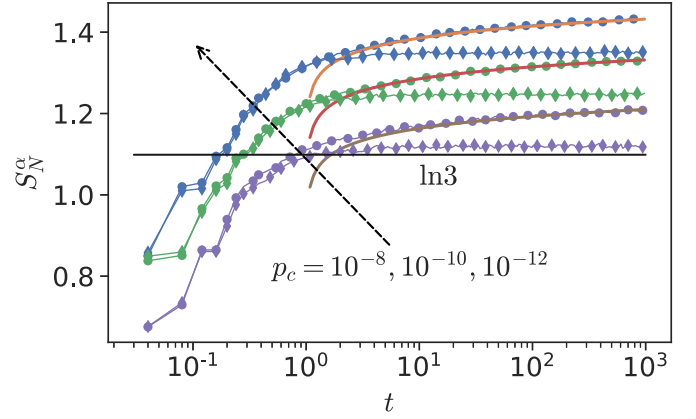
growth of number fluctuations, reflected in the ln ln t scaling of the number entropy, the probabilities for large number fluctuations will remain very small for numerically accessible timescales. Nevertheless, these fluctuations will eventually become large and destroy localization if they continue to grow. It is thus important to consider a quantity that is sensitive also to the tails of the number distributions. A potential candidate for such a quantity is the Hartley number entropy which is the Rényi entropy, Eq. (2), of degree $\alpha = 0$. The Hartley entropy is the logarithm of the cardinality of $p(n)$, i.e., it counts the number of configurations with probabilities different from zero.

Since quantum mechanically the unitary time evolution immediately leads to a nonzero probability for any particle distribution (although most of them will be extremely small) consistent with total particle number conservation independent of whether or not the system is localized, it is important to introduce a cutoff p_c and to only consider configurations with $p(n, t) > p_c$. All values below the cutoff are set to zero, and the distribution is renormalized. The important point then is that for a localized system this truncated Hartley number entropy with *any* cutoff $p_c > 0$ has to saturate in the thermodynamic limit, i.e., there can only be a finite number of configurations with $p(n) > p_c$ for long times. The saturation value will, of course, depend on the cutoff p_c.

We here choose a very small but nonvanishing value of α and calculate the time evolution of $S_N^{(0.001)}$. The results for the Hartley entropy are shown in Fig. 5(b) for $p_c = 10^{-10}$. For each disorder realization, $p(n, t = 0) = 1$ for n corresponding to the initial number of particles in the partition and zero otherwise. The truncated Hartley entropy for each realization—and, consequently, also the average—is therefore zero at $t = 0$. The entropy then continues to increase $\sim \ln \ln t$ well above the value of ln 3. Even more importantly, we do not find any signatures for a saturation for all numerically accessible times. Also shown is the result for the Anderson case, i.e., Eq. (3) with $V = 0$. Here the Hartley entropy saturates, which is consistent with a strict localization of particles. Figure 6 shows that whereas the values of the entropies for the MBL
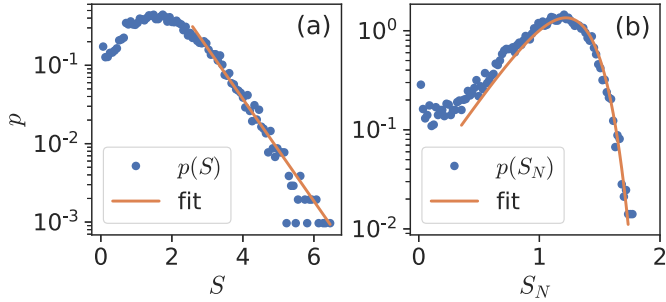
FIG. 7. Distribution of saturation values for the free fermion model with off-diagonal disorder, Eq. (A1), for $L = 1024$ using 20 000 disorder realizations: (a) von Neumann entropy and (b) number entropy. Symbols represent numerical data, the line in (a) is an exponential fit $p(S) \sim e^{-(3/2)S}$, and the line in (b) is the corresponding fit for S_N using the relation (4), $p(S_N) \sim \exp[4(S_N - \gamma)]\exp\{-\frac{3}{2}\exp[4(S_N - \gamma)]\}$ with $\gamma = \ln 3.75$. Here the constants are fit parameters.

and Anderson case do depend on the chosen cutoff p_c, the qualitative behavior is independent of p_c.

We can define the occupied particle number state $\tilde{n}(p_c)$ which is furthest away from the most likely value $n_{\max}$ while still obeying $p(\tilde{n}) \geqslant p_c$. The dynamical behavior of the truncated Hartley number entropy, shown in Fig. 5, must then be understood as an increase in $\tilde{n}$ according to

$$\tilde{n} \sim (\ln t)^\beta, \tag{7}$$

where $\beta \leqslant \frac{1}{2}$. In other words, the width of $p(n)$ measured at p_c is increasing logarithmically in time. This must be interpreted as a constant flow of probability to higher particle number fluctuations.

V. CONCLUSIONS

We have presented a detailed study of particle number fluctuations in the putative MBL phase of the isotropic Heisenberg model. Our results indicate that particles continue to spread through the system at a very slow rate even for strong disorder, far from the ergodic-MBL transition. Our conclusions are based on two main findings: (1) For all disorder strengths $D > D_c$ investigated, the time regime where $S \sim \ln t$ holds in a finite system is exactly the same where $S_N \sim \ln \ln t$ holds. A saturation of $S_N(t)$ while $S(t)$ continues to grow is never observed. We have also shown that the growth of S_N is not a consequence of rare regions but rather represents typical behavior. (2) For all disorder strengths $D > D_c$ investigated, the Hartley number entropy grows as $S_N^{(\alpha \to 0)} \sim \ln \ln t$ and reaches value larger than $\ln 3$. The width of the distribution $p(n)$ measured at some small cutoff p_c thus grows $\sim \ln t$: There is a constant probability flow towards higher particle number fluctuations. The system seems to be able to access all allowed particle distributions at long times in the thermodynamic limit, which would be inconsistent with localization.

In addition, we have also shown that the sharp cutoff in the distributions of number entropies at $S_N \sim \ln 3$ observed in Ref. [27] does not contradict the relation $S \sim \exp(S_N)$ established in Refs. [24,25] but is rather fully consistent with it. Other arguments in favor of a full localization given in Ref. [27] were based on a study of the saturation values of
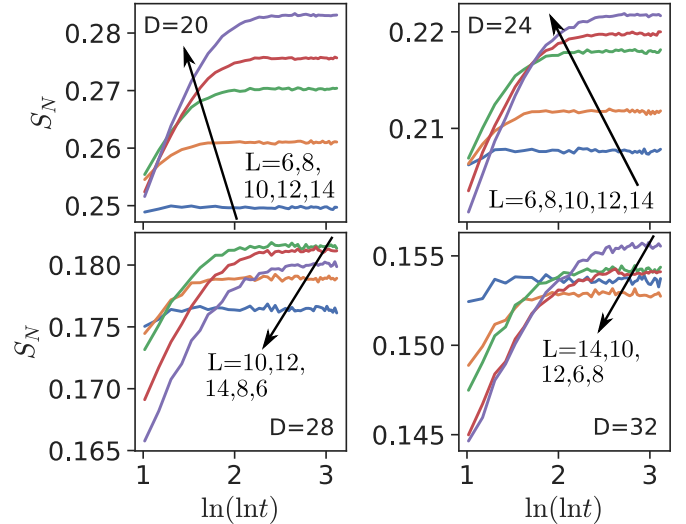

FIG. 8. $S_N(t)$ as a function of $\ln \ln t$ for $L = 6, 8, 10, 12, 14$, and different D's. The saturation values show no clear consistent scaling with system size. Note, in particular, that the saturation values scale nonmonotonically with L for $D = 28, 32$.

S_N. This quantity, however, is difficult to analyze because the long saturation times for large systems are causing numerical issues, the lack of a known scaling, and the possible nonmonotonicity of the saturation values as a function of system size. These issues are discussed further in Appendix B.

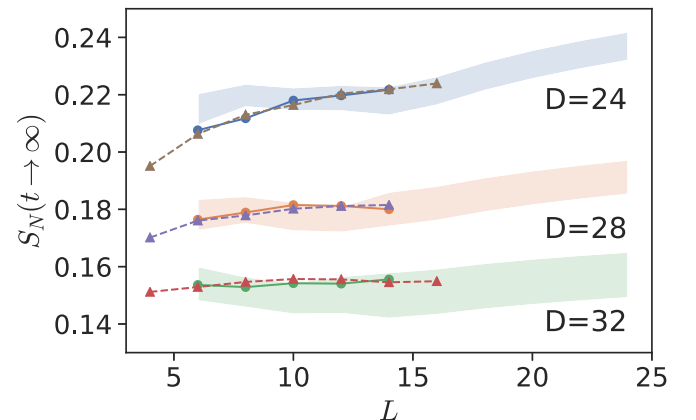FIG. 9. Estimates for the saturation values of $S_N(t \to \infty)$. For system sizes up to $L = 14$, the saturation values are obtained directly from exact diagonalizations (full circles) and compared to the values from Ref. [27] (triangles) for disorder strengths $D = 24, 28$, and 32. For larger system sizes the method described in the text is used, leading to the shaded bands.

APPENDIX A: $p(S_N)$ FOR FREE FERMIONS WITH OFF-DIAGONAL DISORDER

Here we want to demonstrate that also for exactly solvable models which are known to *not* fully localize, the probability distribution of the number entropy has a seemingly sharp decline. To this end, we consider free fermions on a lattice with off-diagonal (bond) disorder,

$$H = -\sum_j J_j(c_j^\dagger c_{j+1} + \text{H.c.}), \tag{A1}$$

where the random hopping amplitudes J_j are drawn from a box distribution. For this model all properties can be calculated from the single-particle correlation matrix allowing to study very large system sizes. It is known that the model is critical with a localization length that diverges at zero energy. This leads to the interesting scalings [24,47] $S \sim \ln \ln t$ and $S_N \sim \ln \ln \ln t$. Despite the fact that this model is known to not fully localize, the probability distributions of the entanglement entropy and the number entropy show qualitatively the same behavior as for the disordered Heisenberg chain found in Ref. [27]. In particular, $p(S_N)$ has a sharp drop off. This is illustrated in Fig. 7.

APPENDIX B: SATURATION VALUES OF ENTROPIES

Here we want to address the question of what information can be obtained from trying to extrapolate the saturation values of the number entropy in system size. We will demonstrate that no clear scaling law emerges from numerical simulations for the available system sizes. Note that the scaling function is not known *a priori*.

We start by showing in Fig. 8 the results for $S_N(t)$ for four different disorder strengths and various system sizes. By comparing the different disorder strengths, it is obvious that there is no simple scaling function $f(D, L)$ of the saturation values as a function of system size L and disorder strength D. Second, the scaling in system size is not monotonic for $D = 28, 32$. I.e., the saturation value as a function of system size can show a "dip" which is not indicative of the thermodynamic limit, making any extrapolation difficult. Finally, we note that the saturation times are roughly increasing exponentially with system size and already reach times $\sim 10^9$ for $L = 14$. Since the calculations are performed in double precision, times $t \gtrsim 10^{14}$ are not accessible, and averaging over times beyond what is reliably possible in double precision can potentially lead to incorrect results. Overall, it appears to be very difficult to make any reliable statements about the scaling of the saturation values of the number entropy based on exact diagonalizations of small systems in double precision at very large disorder.

Our best try to estimate the saturation values for system sizes up to $L = 24$ is shown in Fig. 9. For system sizes $L > 14$ we proceed as follows: First, we extrapolate the saturation times $t_{\text{sat}} \sim \exp(L)$, obtained for smaller system sizes, in L, see the Supplemental Material of Ref. [25]. Second, the double logarithmic fit of S_N obtained for smaller times is used to determine the saturation value of $S_N(t \to \infty) \approx (\nu/2) \ln \ln t_{\text{sat}} + b$. This leads to the shaded bands with the width of the shaded bands being a consequence of the uncertainty in estimating t_{sat}, ν, and b. As we have already seen in Fig. 8 for smaller system sizes, the scaling of the saturation value with L is, in general, nonmonotonic. We note, in particular, that also for $D = 32$ the saturation value appears to *increase* for system sizes $L \gtrsim 16$. We, thus, believe that the interpretation in Ref. [27] of the decrease in the saturation values in a certain range of system sizes as an indication of a saturation in the thermodynamic limit is not justified.

A more useful approach—less prone to issues with the finite-size scaling—is to study the dependence of the timescale where S (S_N) start to deviate from a logarithmic (log-log) scaling. This point has been investigated in Sec. II A of the main text, and the corresponding timescales are indicated in Fig. 2 in the same section.

[1] P. W. Anderson, Absence of diffusion in certain random lattices, Phys. Rev. **109**, 1492 (1958).

[2] E. Abrahams, P. W. Anderson, D. C. Licciardello, and T. V. Ramakrishnan, Scaling Theory of Localization: Absence of Quantum Diffusion in Two Dimensions, Phys. Rev. Lett. **42**, 673 (1979).

[3] *50 Years of Anderson Localization*, edited by E. Abrahams (World Scientific, Singapore, 2010).

[4] D. M. Basko, I. L. Aleiner, and B. L. Altshuler, Metal-insulator transition in a weakly interacting many-electron system with localized single-particle states, Ann. Phys. **321** 1126 (2006).

[5] V. Oganesyan and D. A. Huse, Localization of interacting fermions at high temperature, Phys. Rev. B **75**, 155111 (2007).

[6] A. Pal and D. A. Huse, Many-body localization phase transition, Phys. Rev. B **82**, 174411 (2010).

[7] D. J. Luitz, N. Laflorencie, and F. Alet, Many-body localization edge in the random-field Heisenberg chain, Phys. Rev. B **91**, 081103(R) (2015).

[8] D. J. Luitz, N. Laflorencie, and F. Alet, Extended slow dynamical regime close to the many-body localization transition, Phys. Rev. B **93**, 060201(R) (2016).

[9] R. Nandkishore and D. A. Huse, Many-body localization and thermalization in quantum statistical mechanics, Annu. Rev. Condens. Matter Phys. **6**, 15 (2015).

[10] E. Altman and R. Vosk, Universal dynamics and renormalization in many-body-localized systems, Annu. Rev. Condens. Matter Phys. **6**, 383 (2015).

[11] M. Serbyn, Z. Papić, and D. A. Abanin, Local Conservation Laws and the Structure of the Many-Body Localized States, Phys. Rev. Lett. **111**, 127201 (2013).

[12] Y. Bar Lev, G. Cohen, and D. R. Reichman, Absence of Diffusion in an Interacting System of Spinless Fermions on a One-Dimensional Disordered Lattice, Phys. Rev. Lett. **114**, 100601 (2015).

[13] R. Vosk, D. A. Huse, and E. Altman, Theory of the Many-Body Localization Transition in One-Dimensional Systems, Phys. Rev. X **5**, 031032 (2015).

[14] A. C. Potter, R. Vasseur, and S. A. Parameswaran, Universal Properties of Many-Body Delocalization Transitions, Phys. Rev. X **5**, 031033 (2015).

[15] R. Vosk and E. Altman, Many-Body Localization in One Dimension as a Dynamical Renormalization Group Fixed Point, Phys. Rev. Lett. **110**, 067204 (2013).

[16] R. Vosk and E. Altman, Dynamical Quantum Phase Transitions in Random Spin Chains, Phys. Rev. Lett. **112**, 217204 (2014).

[17] F. Pietracaprina, N. Macé, D. J. Luitz, and F. Alet, Shift-invert diagonalization of large many-body localizing spin chains, SciPost Phys. **5**, 045 (2018).

[18] V. Ros, M. Müller, and A. Scardicchio, Integrals of motion in the many-body localized phase, Nucl. Phys. B **891**, 420 (2014).

[19] J. Z. Imbrie, Diagonalization and Many-Body Localization for a Disordered Quantum Spin Chain, Phys. Rev. Lett. **117**, 027201 (2016).

[20] J. Suntajs, J. Bonca, T. Prosen, and L. Vidmar, Quantum chaos challenges many-body localization, Phys. Rev. E **102**, 062144 (2020).

[21] J. Suntajs, J. Bonca, T. Prosen, and L. Vidmar, Ergodicity breaking transition in finite disordered spin chains, Phys. Rev. B **102**, 064207 (2020).

[22] M. Žnidarič and M. Ljubotina, Interaction instability of localization in quasiperiodic systems, Proc. Natl. Acad. Sci. USA **115**, 4595 (2018).

[23] D. Sels and A. Polkovnikov, Dynamical obstruction to localization in a disordered spin chain, arXiv:2009.04501.

[24] M. Kiefer-Emmanouilidis, R. Unanyan, J. Sirker, and M. Fleischhauer, Bounds on the entanglement entropy by the number entropy in non-interacting fermionic systems, SciPost Phys. **8**, 083 (2020).

[25] M. Kiefer-Emmanouilidis, R. Unanyan, M. Fleischhauer, and J. Sirker, Evidence for Unbounded Growth of the Number Entropy in Many-Body Localized Phases, Phys. Rev. Lett. **124**, 243601 (2020).

[26] D. A. Abanin, J. H. Bardarson, G. De Tomasi, S. Gopalakrishnan, V. Khemani, S. A. Parameswaran, F. Pollmann, A. C. Potter, M. Serbyn, and R. Vasseur, Distinguishing localization from chaos: Challenges in finite-size systems, arXiv:1911.04501.

[27] D. J. Luitz and Y. B. Lev, Absence of slow particle transport in the many-body localized phase, Phys. Rev. B **102**, 100202(R) (2020).

[28] P. Sierant, D. Delande, and J. Zakrzewski, Thouless Time Analysis of Anderson and Many-Body Localization Transitions, Phys. Rev. Lett. **124**, 186601 (2020).

[29] P. Sierant, M. Lewenstein, and J. Zakrzewski, Polynomially Filtered Exact Diagonalization Approach to Many-Body Localization, Phys. Rev. Lett. **125**, 156601 (2020).

[30] J. Léonard, M. Rispoli, A. Lukin, R. Schittko, S. Kim, J. Kwan, D. Sels, E. Demler, and M. Greiner, Signatures of bath-induced quantum avalanches in a many-body–localized system, arXiv:2012.15270.

[31] H. M. Wiseman and J. A. Vaccaro, Entanglement of Indistinguishable Particles Shared between Two Parties, Phys. Rev. Lett. **91**, 097902 (2003).

[32] T. Rakovszky, C. W. von Keyserlingk, and F. Pollmann, Entanglement growth after inhomogenous quenches, Phys. Rev. B **100**, 125139 (2019).

[33] A. Lukin, M. Rispoli, R. Schittko, M. E. Tai, A. M. Kaufman, S. Choi, V. Khemani, J. Leonard, and M. Greiner, Probing entanglement in a many-body-localized system, Science **364**, 256 (2019).

[34] R. Bonsignori, P. Ruggiero, and P. Calabrese, Symmetry resolved entanglement in free fermionic systems, J. Phys. A: Math. Theor. **52**, 475302 (2019).

[35] S. Murciano, G. D. Giulio, and P. Calabrese, Symmetry resolved entanglement in gapped integrable systems: a corner transfer matrix approach, SciPost Phys. **8**, 46 (2020).

[36] S. Murciano, G. D. Giulio, and P. Calabrese, Entanglement and symmetry resolution in two dimensional free quantum field theories, J. High Energy Phys. 08 (2020) 073.

[37] N. Schuch, F. Verstraete, and J. I. Cirac, Nonlocal Resources in the Presence of Superselection Rules, Phys. Rev. Lett. **92**, 087904 (2004).

[38] N. Schuch, F. Verstraete, and J. I. Cirac, Quantum entanglement theory in the presence of superselection rules, Phys. Rev. A **70**, 042310 (2004).

[39] K. Monkman and J. Sirker, Operational entanglement of symmetry-protected topological edge states, Phys. Rev. Res. **2**, 043191 (2020).

[40] M. Žnidarič, T. Prosen, and P. Prelovšek, Many-body localization in the Heisenberg XXZ magnet in a random field, Phys. Rev. B **77**, 064426 (2008).

[41] J. H. Bardarson, F. Pollmann, and J. E. Moore, Unbounded Growth of Entanglement in Models of Many-Body Localization, Phys. Rev. Lett. **109**, 017202 (2012).

[42] F. Andraschko, T. Enss, and J. Sirker, Purification and Many-Body Localization in Cold Atomic Gases, Phys. Rev. Lett. **113**, 217201 (2014).

[43] T. Enss, F. Andraschko, and J. Sirker, Many-body localization in infinite chains, Phys. Rev. B **95**, 045121 (2017).

[44] R. Singh, J. H. Bardarson, and F. Pollmann, Signatures of the many-body localization transition in the dynamics of entanglement and bipartite fluctuations, New J. Phys. **18**, 023046 (2016).

[45] S. Gopalakrishnan, M. Müller, V. Khemani, M. Knap, E. Demler, and D. A. Huse, Low-frequency conductivity in many-body localized systems, Phys. Rev. B **92**, 104202 (2015).

[46] K. Agarwal, E. Altman, E. Demler, S. Gopalakrishnan, D. A. Huse, and M. Knap, Rare-region effects and dynamics near the many-body localization transition, Ann. Phys. (NY) **529**, 1600326 (2017).

[47] Y. Zhao, F. Andraschko, and J. Sirker, Entanglement entropy of disordered quantum chains following a global quench, Phys. Rev. B **93**, 205146 (2016).

[48] M. Suzuki, Generalized trotter's formula and systematic approximants of exponential operators and inner derivations with

applications to many-body problems, Commun. Math. Phys. **51**, 183 (1976).

[49] M. Suzuki, Transfer-matrix method and monte carlo simulation in quantum spin systems, Phys. Rev. B **31**, 2957 (1985).

[50] H. F. Trotter, On the product of semi-groups of operators, Proc. Amer. Math. Soc. **10**, 545 (1959).

[51] D. A. Abanin, E. Altman, I. Bloch, and M. Serbyn, Colloquium: Many-body localization, thermalization, and entanglement, Rev. Mod. Phys. **91**, 021001 (2019).